Control Strategy for the Stable Operation of Multilevel Converter Topologies in DG Technology

Edris Pouresmaeil
Centre for Smart Energy Solutions,
Uni. Of Southern Denmark, Odense, Denmark
edp@iti.sdu.dk

Majid Mehrasa
Babol (Noshirvani) University of Technology, Babol, Iran
m.majidmehrasa@gmail.com

João P. S. Catalão
Uni. Beira Interior, Covilha, INESC-ID, and IST, Univ. Lisbon, Portugal
catalao@ubi.pt

***Abstract*—A control technique of multilevel converter topologies based on Direct Lyapunov Control method is presented in this paper for integration of Distributed Generation (DG) resources into the power grid. The compensation of instantaneous variations in the reference current components in *ac*-side and *dc*-voltage variations of cascaded capacitors in *dc*-side of the interfacing system are considered properly, which is the main contribution and novelty of this work in comparison with other control strategies. The proposed control technique provides the continuous injection of active power in fundamental frequency from DG sources to the grid. In addition, reactive power and harmonic current components of loads are provided with a fast dynamic response; thereby, achieving sinusoidal grid currents in phase with load voltages, while the required power from load side is more than the maximum capacity of interfaced converter, is possible. Simulation results confirm the effectiveness of the proposed control strategy in DG technology during dynamic and steady-state operating conditions.**

***Keywords*—Distributed Generation (DG), Direct Lyapunov Method (DLM), Energy Management, Multilevel Converter.**

I. NOMENCLATURE

A. Indices

i	a,b,c
j	1,2

B. Abbreviations

CC	Capability Curve
DG	Distributed Generation
DLM	Direct Lyapunov Method
KVL	Kirchhoff's Voltage Law
KCL	Kirchhoff's Current Law
LPF	Low Pass Filter
NPC	Neutral Point Clamped
PCC	Point of Common Coupling
PF	Power Factor
THD	Total Harmonic Distortion
VSC	Voltage Source Converter

C. Variables

i_{g_i}	Grid Currents
i_{l_i}	Load Currents
i_{ci}	DG Currents
i_d	Current Components d-axis
i_q	Current Components q-axis
i_{dc}	*dc* Current
I_{dc}	Steady state value of *dc* Current
I_{refd}	Reference current of DG in d-axis
I_{refq}	Reference current of DG in q-axis
i_{dhn}	Load current components in harmonic frequencies
v_{dc}	*dc*-link voltage
v_{gi}	Grid voltage
v_{pcci}	Voltage at PCC
v_m	Reference voltage vector at PCC
v_{pccd}	Load voltage in d-axis
v_{pccq}	Load voltage in q-axis
v_{cj}	Switching state function
v_{cs}	*dc*-link voltages on the cascaded capacitors
U_{eqj}	Switching state function
U_{abc}	Equivalent voltage vectors at PCC Grid voltage
S_{abc}	Equivalent switching functions at PCC
S_{ij}	Switching of transistors in each phase

D. Parameters

R_c	Equivalent resistance of the *ac* filter, coupling transformer, and connection cables
L_c	Equivalent inductance of the *ac* filter, coupling transformer, and connection cables
R_g	Grid resistance up to the PCC
L_g	Grid inductance up to the PCC
R_{abc}	Resistance matrix of the DG model
L_{abc}	Inductance matrix of the DG model
C_j	Cascaded *dc* capacitors
P_{DG}	Reference active power of DG
P_{max}	Maximum active power of DG
Q_{DG}	Reference reactive power of DG
Q_l	Load reactive power
ω	Grid angular frequency
α_j	Constant coefficient of switching function in dynamic state operation
β_j	Constant coefficient of switching function in dynamic state operation
f	Fundamental frequency
f_c	Cut-off frequency

II. INTRODUCTION

Distributed Generation (DG) technology refers to any electric power generation technology that is on-site or close to the load center [1].

DG sources based on renewable energy are seen as a reliable alternative to the traditional energy sources based on fossil fuel sources.

The electricity business restructuring and necessity of producing more electricity [2], combined with environmental regulations due to greenhouse gas emissions [3], and the recent improvements in small scale power generation are the main factors driving the energy sector into a new era of power generation, where large portions of increases in electrical energy demand will be met through widespread installation of energy sources or what's known as DG sources [4].

DG has the potential of being less costly, more efficient, more reliable, and facilitates the generation of electricity in proximity to load centers, where rural and household consumers are the cases that are mostly concerned with it. In addition, it can give industrial consumers various options in a wider range of high reliability and low price combinations [5]. However, the increasing number of DG units in the electrical network requires new techniques for the operation and management of the network, in order to maintain or even to improve the power supply reliability and quality in the future. As a consequence, a control technique for power management in the network becomes of high interest in this technology [6], [7]. Normally, a Voltage Source Converter (VSC) is proposed for the interfacing between DG sources and the utility grid, and multilevel converters are a good trade-off solution between performance and cost in high-power systems. The main advantages of multilevel converters are reduced voltage ratings for the switches, good harmonic spectrum, and good dynamic response; however, the control complexities increase in this topology [8].

Several studies have been reported in the literature regarding the control of multilevel converter topologies, and in each control strategy a solution for a problem in the power network has been discussed [9]. In this paper, a control plan for the multilevel converter topologies based on Direct Lyapunov Method (DLM) is proposed for the interconnection of DG sources to the grid [10]. A compensation technique for the instantaneous variation of reference current components in the *ac*-side and *dc*-voltage variations of cascaded capacitors in the *dc*-side of interfaced converter are considered precisely, which is the main contribution and novelty of this work in comparison with other potential control strategies.

The rest of the paper is organized into four sections. Following the introduction, general schematic diagram of the proposed DG model will be introduced in Section III and the dynamic and steady state analysis of this model will be elaborated properly. Application of DLM technique for the control and stable operation of DG interface system will be presented in section IV. Moreover, simulation results are performed to demonstrate the efficiency and applicability of the developed control strategy in Section V. Finally, conclusions are drawn in Section VI.

III. PROPOSED DG MODEL

Fig. 1 illustrates the schematic diagram of the proposed DG model, where conventional signs of voltage and current components are indicated in this schema. In addition, the DG source and additional components are represented as a *dc* current source that is connected to the *dc* side of the converter.

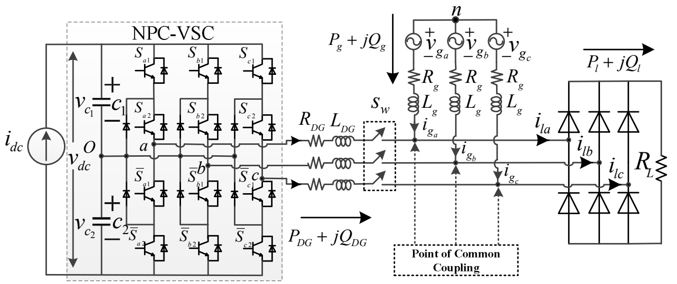

Fig. 1. Functional diagram of the proposed model.

A. Dynamic Model Analysis of the Proposed Model

To draw an appropriate plan to control the integration of DG sources to the power grid, a dynamic analytical model of the proposed model should be developed. According to Fig. 1, KVL and KCL laws for the voltage at PCC and current in *dc* side of interfaced converter leads in,

$$\begin{aligned} &L_c \frac{di_{c_a}}{dt} + R_c i_{c_a} + v_{pcc_a} = v_{ka} + v_{kn} = v_a \\ &L_c \frac{di_{c_b}}{dt} + R_c i_{c_b} + v_{pcc_b} = v_{kb} + v_{kn} = v_b \\ &L_c \frac{di_{c_c}}{dt} + R_c i_{c_c} + v_{pcc_c} = v_{kc} + v_{kn} = v_c \\ &C \frac{dv_{c_1}}{dt} + \left(S_{a_1} i_{c_a} + S_{b_1} i_{c_b} + S_{c_1} i_{c_c} \right) - i_{dc} = 0 \\ &C \frac{dv_{c_2}}{dt} - \left(\left(1 - S_{a_2}\right) i_{c_a} + \left(1 - S_{b_2}\right) i_{c_b} + \left(1 - S_{c_2}\right) i_{c_c} \right) - i_{dc} = 0 \end{aligned} \tag{1}$$

By substituting the relation between load voltages and switching functions of the proposed converter in (1), voltage relation between *ac* and *dc* sides of the interfacing system can be mentioned as,

$$v_i = \left(S_{i_1} - \frac{1}{3} \sum_{n=a}^{b,c} S_{n_1} \right) v_{c_1} + \left(S_{i_2} - \frac{1}{3} \sum_{n=a}^{b,c} S_{n_2} \right) v_{c_2} \tag{2}$$

By referring to (2), equivalent switching functions in the interfacing system can be obtained as,

$$\begin{aligned} u_{eq_{i1}} &= -\left(S_{i_1} - \frac{1}{3} \sum_{n=a}^{b,c} S_{n_1} \right) \\ u_{eq_{i2}} &= -\left(S_{i_2} - \frac{1}{3} \sum_{n=a}^{b,c} S_{n_2} \right) \end{aligned} \tag{3}$$

Eq. (3) demonstrates that the equivalent switching functions are depended on the switching of S_{ij}, completely describing the behavior of each leg in interfaced converter. By substituting (3) in (1), dynamic model of the system can be expressed as,

$$L_{abc} \frac{dI_{abc}}{dt} + R_{abc} I_{abc} + U_{abc_1} v_{c_1} + U_{abc_2} v_{c_2} + S_{abc} = 0 \tag{4}$$

B. Steady State Analysis of the Proposed Model

By the use of Park transformation matrix, the dynamic model in (4) can be transformed to *dq* frame. All the alternative variables in main frequency are converted to *dc* value; thus, controlling and filtering will be achieved easier [11].

Then, dynamic model of the system in *dq* frame can be expressed as,

$$
\begin{aligned}
&L_c \frac{di_{c_d}}{dt} + R_c i_{c_d} - \omega L_c i_{c_q} + v_{c_1} u_{eq_{d1}} + v_{c_2} u_{eq_{d2}} + v_{pcc_d} = 0 \\
&L_c \frac{di_{c_q}}{dt} + R_c i_{c_q} + \omega L_c i_{c_d} + v_{c_1} u_{eq_{q1}} + v_{c_2} u_{eq_{q2}} + v_{pcc_q} = 0 \\
&C \frac{dv_{c_1}}{dt} - \left(u_{eq_{d1}} i_{c_d} + u_{eq_{q1}} i_{c_q} \right) - i_{dc} = 0 \\
&C \frac{dv_{c_2}}{dt} - \left(u_{eq_{d2}} i_{c_d} + u_{eq_{q2}} i_{c_q} \right) - i_{dc} = 0
\end{aligned} \tag{5}
$$

Equation (5) illustrates the dynamic equation of the proposed DG model in *dq* frame, which is used for the dynamic and steady state analysis of the model.

IV. Proposed Control Technique

The proposed control technique is based on DLM, which is an appropriate technique for studying the stability of the proposed model in the electrical network [12].

By the proposed control technique, DG becomes strengthened against large signal disturbances and during the presence of unexpected changes in the parameters of the proposed model.

A. Steady State Evaluation in the Control Loop

Assuming that I_{ref_d} and I_{ref_q} are equilibrium points of the proposed DG in *dq* reference frame, if the total harmonic frequencies of active power and the maximum active power at main frequency generated by the DG, reference current in the current control loop of DG can be expressed as,

$$ i_{c_d} = I_{ref_d} \tag{6} $$

By this consideration, the maximum active power of DG in fundamental frequency and harmonic currents of nonlinear loads in d-axis will be injected to the grid. Therefore, if the maximum active power of DG in fundamental frequency was more than the required active power from the load, the injected active power in fundamental and harmonic frequencies from the grid to load will be zero.

On the other hand, in order to generate the total reactive power through the proposed DG, I_{refq} should be considered as,

$$ i_{c_q} = I_{ref_q} \tag{7} $$

Equation (7) leads to the improvement of Power Factor (PF) between load voltage and grid current, and the voltage quality at PCC. Moreover, voltage of load should be balanced and sinusoidal in the steady-state, therefore,

$$ v_{pcc_d} = v_m, \quad v_{pcc_q} = 0 \tag{8} $$

According to (7) and (8), the PF between grid current and load voltage will be unity. Equations (6), (7) and (8) are considered as the steady-state conditions in the proposed model.

By applying these conditions to (5), (9) can be obtained as,

$$
\begin{aligned}
&L_c \frac{dI_{ref_d}}{dt} + R_c I_{ref_d} - \omega L_c I_{ref_q} + v_{c_1} u_{eq_{d1s}} + v_{c_2} u_{eq_{d2s}} + v_m = 0 \\
&L_c \frac{dI_{ref_q}}{dt} + R_c I_{ref_q} + \omega L_c I_{ref_d} + v_{c_1} u_{eq_{q1s}} + v_{c_2} u_{eq_{q2s}} = 0 \\
&u_{eq_{d1s}} I_{ref_d} + u_{eq_{q1s}} I_{ref_q} + I_{dc} = 0 \\
&u_{eq_{d2s}} I_{ref_d} + u_{eq_{q2s}} I_{ref_q} + I_{dc} = 0
\end{aligned} \tag{9}
$$

The average values of instantaneous variations in reference current components of DG control loop are defined as,

$$ \frac{dI_{ref_d}}{dt} = I_{av_d}, \quad \frac{dI_{ref_q}}{dt} = I_{av_q} \tag{10} $$

Also, in the steady state condition $v_{c_1} = v_{c_2} = v_{dc}/2$, $u_{eq_{d1s}} = u_{eq_{d2s}} = u_{eq_{ds}}$ and $u_{eq_{q1s}} = u_{eq_{q2s}} = u_{eq_{qs}}$; then, (11) can be expressed as,

$$
\begin{aligned}
&L_c I_{av_d} + R_c I_{ref_d} - \omega L_c I_{ref_q} + v_{dc} u_{eq_{ds}} + v_m = 0 \\
&L_c I_{av_q} + R_c I_{ref_q} + \omega L_c I_{ref_d} + v_{dc} u_{eq_{qs}} = 0 \\
&u_{eq_{ds}} I_{ref_d} + u_{eq_{qs}} I_{ref_q} + I_{dc} = 0
\end{aligned} \tag{11}
$$

Based on (11), the switching state functions of the interfacing system for the steady state operating condition can be expressed as,

$$ u_{eq_{ds}} = \frac{-v_m - L_c I_{av_d} - R_c I_{ref_d} + \omega L_c I_{ref_q}}{v_{dc}} \tag{12} $$

$$ u_{eq_{qs}} = \frac{-L_c I_{av_q} - R_c I_{ref_q} - \omega L_c I_{ref_d}}{v_{dc}} \tag{13} $$

Equations (12) and (13) can be used for the desired control of DG in the steady state condition by the proper selection of I_{refd} and I_{refq}. Each DG model has a limited capacity for the injection of active and reactive power, so considering the capacity of DG in the design of the control loop for the interfacing system will help to improve the performance of DG model in the distribution grid. By substituting (12) and (13) in the last part of (11), (14) can be obtained as,

$$
\begin{aligned}
&\left(I_{ref_d} + \frac{L_c \mathrm{I}_{av_d} + v_m}{2R_c} \right)^2 + \left(I_{ref_q} + \frac{L_c \mathrm{I}_{av_q}}{2R_c} \right)^2 \\
&= \frac{\left(L_c \mathrm{I}_{av_d} + v_m \right)^2 + \left(L_c \mathrm{I}_{av_q} \right)^2 + 4R_c v_{dc} I_{dc}}{4R_c^2}
\end{aligned} \tag{14}
$$

By multiplying v_m^2 to (14), (15) can be expressed as,

$$
\begin{aligned}
&\left(P_{DG} + \frac{L_c \mathrm{I}_{av_d} v_m + v_m^2}{2R_c} \right)^2 + \left(Q_{DG} - \frac{L_c \mathrm{I}_{av_q} v_m}{2R_c} \right)^2 \\
&= \frac{\left(L_c \mathrm{I}_{av_d} v_m + v_m^2 \right)^2 + \left(L_c \mathrm{I}_{av_q} v_m \right)^2 + 4R_c v_{dc} I_{dc} v_m^2}{4R_c^2}
\end{aligned} \tag{15}
$$

As shown in Fig. 2, (15) is the equation of a circle with the center of C and radius of R. Fig. 2 is known as capability curve (CC) of the proposed DG model, and provides a proper division of active and reactive power between DG and the grid for supplying the load. As can be seen from Fig.2, total reactive power of Load1 can be supplied by DG; but, after connection of Load2 to the grid, total required power from the loads is more than the maximum capacity of DG; then, rest of the active and reactive power will be supplied through the utility grid. Therefore, DG can enhance the quality of grid currents and PF when the load reactive power exists inside the circle. Also, DG can inject the total active power of the load and make the grid current to zero value when the active power exists inside the circle; otherwise, the rest of the active power will be injected from the grid side to the load.

B. Dynamic Evaluation of DLM Technique

Total saved energy ($H(x_1,x_2,x_3,x_4)$) of DG should be calculated in order to study the stability of DG through the DLM and achieving dynamic part of switching functions in the interfaced convertor; thus,

$$H(x_1,x_2,x_3,x_4)=\frac{1}{2}L_c x_1^2+\frac{1}{2}L_c x_2^2+\frac{1}{2}Cx_3^2+\frac{1}{2}Cx_4^2 \tag{16}$$

where, x_1 and x_2 are differences between the reference currents in control loop and injected current by DG ($x=i_{DG}-I_{ref}$), x_3 and x_4 are differences between the voltage of cascaded capacitors generated by DG source and reference *dc* voltages. The globally asymptotically stability against the undesirable disturbances can be achieved for the proposed model if derivative of the total energy of DG in the state variables trajectories becomes definitive negative; then,

$$\frac{d}{dt}H(x_1,x_2,x_3,x_4)=L_c x_1\frac{dx_1}{dt}+L_c x_2\frac{dx_2}{dt}+Cx_3\frac{dx_3}{dt}+Cx_4\frac{dx_4}{dt} \tag{17}$$

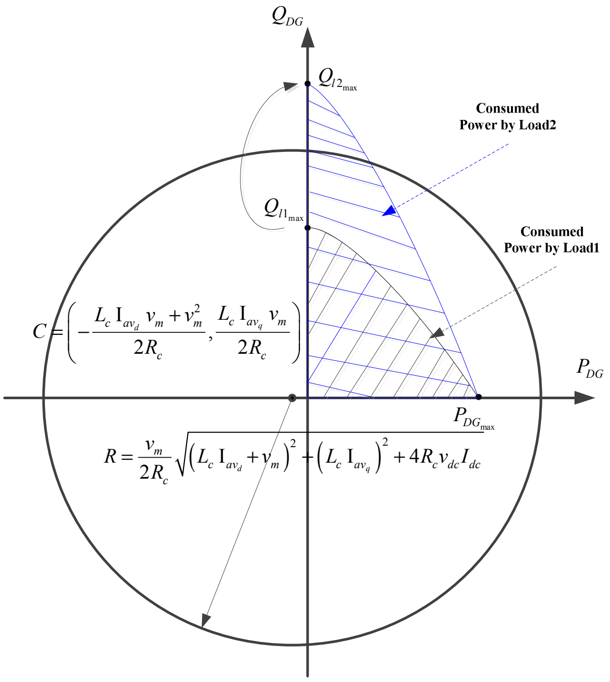

Fig. 2. Capability Curve of the proposed DG model.

The switching state functions are defined as,

$$u_{eq_{dqj}} = u_{eq_{dqjs}} + \Delta u_{eq_{dqj}} \tag{18}$$

where $\Delta u_{eq_{dqj}}$ is the dynamic part of the equivalent switching function of the interfaced converter. Eq. (18) gives equivalent switching functions of the interfaced converter, which include both the dynamic and steady state operating conditions. By substituting steady state conditions of *dc* voltage and switching state functions, and (18) in (5), and considering $x_{dq}=i_{cdq}-i_{refdq}$, (19) and (20) can be obtained as,

$$L_c\frac{dx_1}{dt} = -R_c i_{c_d} + \omega L_c i_{c_q} - L_c I_{av_d} - \left(\frac{v_{c_1}+v_{c_2}}{v_{dc}}\right) \\ \times\left(\omega L_c I_{ref_q} - L_c I_{av_d} - R_c I_{ref_d} - v_m\right) - v_{c_1}\Delta u_{eq_{d1}} - v_{c_2}\Delta u_{eq_{d2}} - v_m \tag{19}$$

$$L_c\frac{dx_2}{dt} = -R_c i_{c_q} - \omega L_c i_{c_d} - L_c I_{av_q} - \left(\frac{v_{c_1}+v_{c_2}}{v_{dc}}\right) \\ \times\left(-\omega L_c I_{ref_d} - L_c I_{av_q} - R_c I_{ref_q}\right) - v_{c_1}\Delta u_{eq_{q1}} - v_{c_2}\Delta u_{eq_{q2}} \tag{20}$$

$$C\frac{dx_3}{dt} = \frac{\left(-L_c I_{av_d} - R_c I_{ref_d} + \omega L_c I_{ref_q} - v_m\right)}{v_{dc}}x_1 \\ +\frac{\left(-L_c I_{av_q} - R_c I_{ref_q} - \omega L_c I_{ref_d}\right)}{v_{dc}}x_2 + \Delta u_{eq_{d1}} i_{c_d} \\ +\Delta u_{eq_{q1}} i_{c_q} + \left(i_{dc} - I_{dc}\right) \tag{21}$$

$$C\frac{dx_4}{dt} = \frac{\left(-L_c I_{av_d} - R_c I_{ref_d} + \omega L_c I_{ref_q} - v_m\right)}{v_{dc}}x_1 \\ +\frac{\left(-L_c I_{av_q} - R_c I_{ref_q} - \omega L_c I_{ref_d}\right)}{v_{dc}}x_2 + \Delta u_{eq_{d2}} i_{c_d} \\ +\Delta u_{eq_{q2}} i_{c_q} + \left(i_{dc} - I_{dc}\right) \tag{22}$$

By substituting (19)-(22) in (17),

$$\frac{d}{dt}H(x_1,x_2,x_3,x_4) = -R_c\left(i_{c_d} - I_{ref_d}\right)^2 - \\ R_c\left(i_{c_q} - I_{ref_q}\right)^2 - \Delta u_{eq_{d1}}\left(\frac{v_{dc}}{2}i_{c_d} - v_{c_1}I_{ref_d}\right) - \\ \Delta u_{eq_{d2}}\left(\frac{v_{dc}}{2}i_{c_d} - v_{c_2}I_{ref_d}\right) - \Delta u_{eq_{q1}}\left(\frac{v_{dc}}{2}i_{c_q} - v_{c_1}I_{ref_q}\right) \\ -\Delta u_{eq_{q2}}\left(\frac{v_{dc}}{2}i_{c_q} - v_{c_2}I_{ref_q}\right) - \left(i_{dc} - I_{dc}\right)\left(v_{c_1} - \frac{v_{dc}}{2}\right) \\ -\left(i_{dc} - I_{dc}\right)\left(v_{c_2} - \frac{v_{dc}}{2}\right) \tag{23}$$

Eq. (23) should be negative value to reach a globally asymptotical stability in DG during the dynamic changes in the model. To reach this goal, dynamic parts of the switching state functions should be defined as,

$$\Delta u_{eq_{d1}} = \gamma_1\left(\frac{v_{dc}}{2} i_{c_d} - v_{c_1} I_{ref_d}\right) \tag{24}$$

$$\Delta u_{eq_{d2}} = \gamma_2\left(\frac{v_{dc}}{2} i_{c_d} - v_{c_2} I_{ref_d}\right) \tag{25}$$

$$\Delta u_{eq_{q1}} = \lambda_1\left(\frac{v_{dc}}{2} i_{c_q} - v_{c_1} I_{ref_q}\right) \tag{26}$$

$$\Delta u_{eq_{q2}} = \lambda_2\left(\frac{v_{dc}}{2} i_{c_q} - v_{c_2} I_{ref_q}\right) \tag{27}$$

Furthermore, v_{c_j} tend to be equal to $v_{dc} / 2$ for making an appropriate compatibility between the voltage of *dc* and *ac* sides during the integrating time; then, the two last terms in (23) will be eliminated and consequently the value of general equation will be negative.

As a result, application of DLM strategy can guarantee a stable operation for the proposed DG model during dynamic and steady state operating conditions.

The switching functions given in (24) to (27) make a rapid reaction for the proposed control technique; therefore, DG currents follow their reference values with a fast dynamic response in a stable region. The process of switching function generation in DLM technique is depicted in Fig. 3.

C. Reference Current Calculation

Current reference values should be defined based on the objectives of DLM technique for an efficient operation during dynamic and steady states operating conditions. Therefore, the harmonic current components, maximum active power and all the reactive power should be considered in the control loop of the proposed model. By this consideration and based on Fig. 2, rest of the power for the additional load which will be injected from the utility grid as an active power in fundamental frequency.

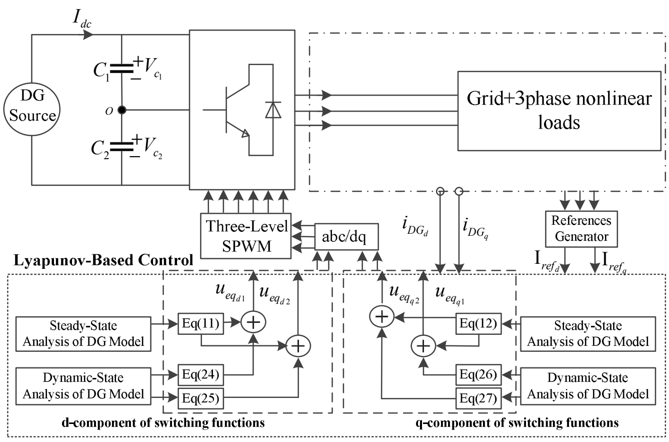

Fig. 3. Block diagram of DLM for the proposed DG model.

Based on the mentioned assumptions, d-component of reference current in the proposed DG link can be achieved by doing the sum of maximum capacity of DG interfacing system for the injection of active power in main frequency and alternative terms of load current components in d-axis as,

$$i^*_{c_d} = \frac{P_{\max}}{v_m} + \sum_{n=2}^{\infty} i_{d_{hn}} = \frac{P_{DG}}{v_{pcc_d}} + i_{l_d}\left(1 - LPF\right) \tag{28}$$

The alternative parts of load current components can be separated from the *dc* part by a Low Pass Filter (LPF). The considered filter has a cut-off frequency fc = (f=2) (f = 50Hz), which promises the extraction of *dc* part from the nonlinear load currents. Moreover, to compensate load reactive power at fundamental and harmonic frequencies, DG must inject i_{l_q} as,

$$i_{l_q} = -\frac{Q_l}{v_m} = -\frac{Q_{DG}}{v_{pcc_d}} = i^*_{c_q} \tag{29}$$

V. SIMULATION RESULTS

The proposed model in Fig.1 has been simulated in Matlab/ Simulink to demonstrate the performance of the proposed DLM in DG technology. The values of model parameters are given in the Appendix.

A 13 kVA NPC VSC has been considered as the heart of the interfacing system between DG source and the utility grid. It is assumed that the interfaced converter generates the maximum power of P=6.5 kW at the main frequency, continuously. Unexpected connection of DG to the grid and load increment is taken into the account in order to evaluate the accurate dynamic response of DLM in the proposed model.

THD analysis of the grid current and analysis of PF between the grid current and load voltage will be evaluated to demonstrate the performance of the proposed control technique in DG technology.

A. DG Connection and Load Increment

Before connection of DG link to the grid, a three phase diode bridge rectifier with resistant load of R = 30 is directly connected to the grid and draws the nonlinear currents from the grid.

At t=0.1 sec, DG is connected to the grid and this procedure continues until t=0.2 sec, while another similar load with resistant of R = 20 is added to the grid.

Fig. 4 depicts the load, grid, and DG currents before and after connection of DG link to the grid, and after additional load increment. As can be seen, before integration of DG to the grid, load is supplied by the utility grid; but, after connection of DG all the current components including the fundamental and harmonic frequencies are injected by DG. After connection of additional load to the grid at t=0.2 sec, the maximum capacity of DG interfaced is less than the total required power of the loads; then, the rest of the power (which is active power in fundamental frequency) is injected by the grid; therefore, load voltage and grid current are in phase during the connection of the additional load to the grid.

Fig. 5 illustrates the active power sharing between the grid, load and DG, before and after integration of DG and before and after additional load increment.

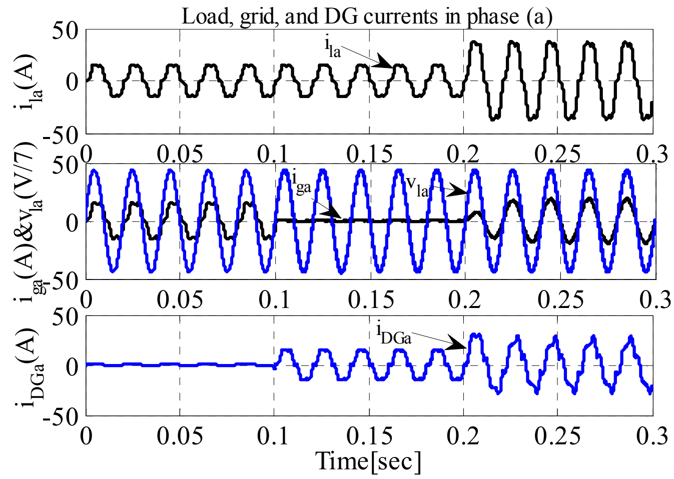

Fig. 4. Load, Grid, and DG currents and load voltage, before and after DG interconnection, and before and after additional load increment.

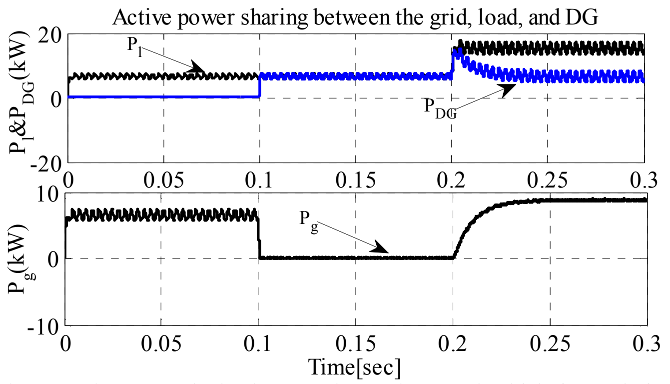

Fig. 5. Active power sharing between the Load, DG and Grid, before and after DG interconnection, and before and after additional load increment.

As shown in Fig. 5, after connection of DG link to the grid, injected power from the grid is reduced to the zero value and load active power in both the fundamental and harmonic frequencies are supplied through DG source. After connection of additional load to the grid at t = 0:2sec, the maximum active power in fundamental frequency and all the harmonic current components are injected via the DG link and the rest of the active power in fundamental frequency is supplied through the main grid.

Reactive power sharing between the grid, load and DG is depicted in Fig. 6.

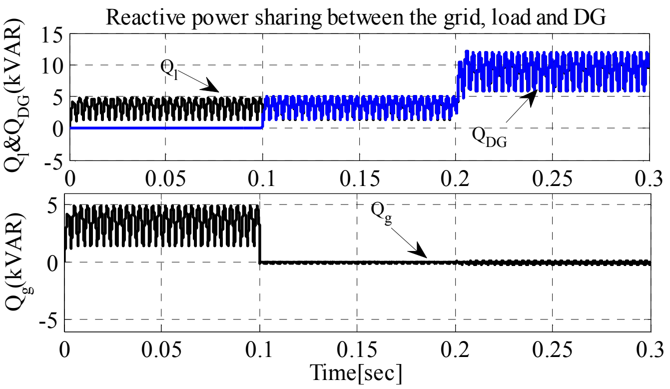

Fig. 6. Reactive power sharing between the Load, DG and Grid, before and after DG interconnection, and before and after additional load increment.

As can be seen in Fig. 6, all the reactive power in both the fundamental and harmonic frequencies are supplied via the DG link after connection of DG source to the grid and before and after connection of additional load to the grid; therefore, utility grid is free of any reactive power components, and load voltage and grid currents are in phase.

B. THD and PF Evaluation

One of the main goals of the DLM strategy is to achieve a unit PF between grid current and load voltage. To reach this goal, total load reactive power should be generated by DG. Fig. 7 indicates the grid current and load voltage in phase (a) during the connection of additional load to the grid. As can be seen, grid current is in phase with load voltage, which confirms a unity value for the PF of the grid. Spectrum analysis results of the load, DG, and grid currents are shown in Fig. 8. As can be seen, THD of load current is 16.7% during the connection of additional load to the grid; but, by interconnection of DG to the grid, THD of grid current is reduced to 1%. The results confirm the capability of the proposed DG model to compensate the harmonic current components of nonlinear loads.

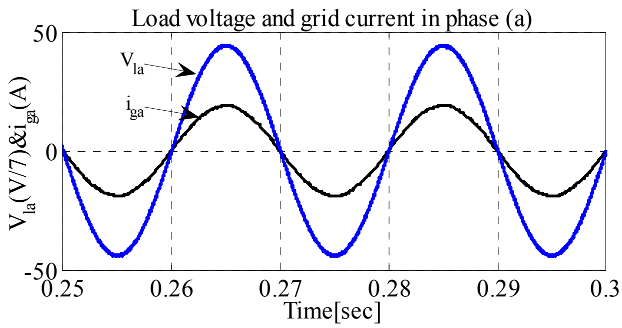

Fig. 7. Grid current and load voltage in phase (a), during load increment.

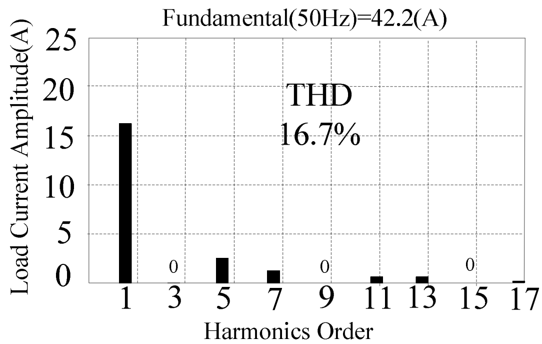

(a)

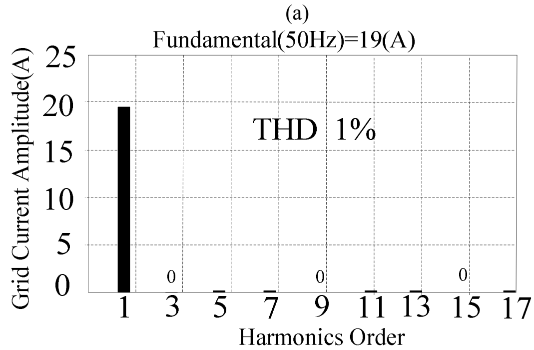

(b)

Fig. 8. Harmonic spectrum of (a) Load current and (b) Grid current, during additional load increment.

VI. CONCLUSION

A robust control technique based on Direct Lyapunov Method was presented in this paper for the control of multilevel converter topologies and integration of DG resources into the power grid. The compensation of instantaneous variations in the reference current components in *ac*- side and *dc*-voltage variations of cascaded capacitors in *dc*-side of the interfacing system was considered properly as the main contribution of this control technique. Simulation results illustrated that in all conditions the maximum active power in fundamental frequency is injected through the DG link to the grid, and the load voltage and grid current are in phase by injection of reactive power of loads in fundamental and harmonic frequencies via the DG link; then, by the improvement of power factor at PCC, DG can act as power factor correction device. In addition, the proposed DG can provide the required harmonic load currents in all conditions; therefore, by reducing the THD of grid current, it can act as an active power filter. The proposed control method can be used for the integration of different types of DG resources particularly based on renewable energy resources for the injection of active and reactive power components in both fundamental and harmonic frequencies simultaneously, which is the main advantage of this control method over other control methods in DG technology.

APPENDIX

Simulation parameters are as follows:

$$v_s = 380V,\ v_{dc} = 1000V,\ f = 50Hz,\ R_c = 0.1m\Omega,\ L_c = 0.45mH,$$
$$\lambda_1, \gamma_1 = 0.01,\ \lambda_2, \gamma_2 = 0.001,\ P_{ref} = 6.5kW.$$

ACKNOWLEDGMENT

This work was supported by FEDER funds (European Union) through COMPETE and by Portuguese funds through FCT, under Projects FCOMP-01-0124-FEDER-020282 (Ref. PTDC/EEA-EEL/118519/2010), PEst-OE/EEI/LA0021/2013. Also, the research leading to these results has received funding from the EU Seventh Framework Programme FP7/2007-2013 under grant agreement no. 309048.

REFERENCES

[1] A. F. Zobaa and C. Cecati, “A comprehensive review on distributed power generation,” in: *Proc. Int. Symposium on Power Electronics, Electrical Drives, Automation and Motion*, pp. 514-518, 2006.

[2] W. Ouyang, H. Cheng, X. Zhang and F. Li, “Evaluation of distributed generation connecting to distribution network based on long-run incremental cost,” *IET Generation, Transmission & Distribution*, vol. 5, no. 5, pp. 561-568, 2011.

[3] M. F. Akorede, H. Hizam, and E. Pouresmaeil, “Distributed energy resources and benefits to the environment,” *Renewable Sustainable Energy Rev.*, vol. 14, no. 2, pp.724-734, 2010.

[4] E. J. Coster, J. M. A. Myrzik, B. Kruimer and W. L. Kling, “Integration issues of distributed generation in distribution grids,” *Proceedings of the IEEE*, vol. 99, no. 1, pp. 28-39, 2011.

[5] C. Chen, S. Duan, T. Cai, B. Liu and G. Hu, “Smart energy management system for optimal microgrid economic operation,” *IET Renewable Power Generation*, vol. 5, no. 3, pp. 258-267, 2011.

[6] E. Pouresmaeil, C. Miguel-Espinar, M. Massot-Campos, D. Montesinos-Miracle, and O. Gomis-Bellmunt, “A control technique for integration of DG units to the electrical networks,” *IEEE Trans. Ind. Electron.*, vol. 60, no. 7, pp. 2881-2893, 2013.

[7] Z. Zeng, H. Yang, R. Zhao and C. Cheng, “Topologies and control strategies of multi-functional grid-connected inverters for power quality enhancement: A comprehensive review,” *Renewable and Sustainable Energy Reviews*, vol. 24, pp. 223-270, 2013.

[8] E. Pouresmaeil, O. Gomis-Bellmunt, D. Montesinos-Miracle, and J. Bergas-Jane, “Multilevel converters control for renewable energy integration to the power grid,” *Energy*, vol. 36, no. 2, pp. 950-963, 2011.

[9] J. Rocabert, A. Luna, F. Blaabjerg and P. Rodriguez, “Control of power converters in AC microgrids,” *IEEE Trans. Power Electron.*, vol. 12, no. 11, pp. 4734-4749, 2012.

[10] S. Rahmani, A. Hamid, and K. Al-Haddad, “A Lyapunov-Function based control for a three-phase shunt hybrid active filter,” *IEEE Trans. Ind. Electron.*, vol. 59, no. 3, pp. 1418-1429, 2012.

[11] E. Pouresmaeil, D. Montesinos-Miracle, O. Gomis-Bellmunt, and J. Bergas-Jane, “A multi-objective control strategy for grid connection of DG (Distributed Generation) resources,” *Energy*, vol. 35, no. 12, pp. 5022-5030, 2010.

[12] M. A. Pai and P. W. Sauer, “ Stability analysis of power systems by Lyapunov’s direct method,” *IEEE Control Systems Magazine*, vol. 9, no.1, pp. 23-27, 1989.